JOURNAL OF AGRICULTURAL AND FOOD CHEMISTRY

Spiro Cross-Links: Representatives of a New Class of Glycoxidation Products

OLIVER REIHL,* KLAUS M. BIEMEL, WOLFGANG EIPPER, MARKUS O. LEDERER, AND WOLFGANG SCHWACK

Institute of Food Chemistry, University of Hohenheim, Garbenstrasse 28, D-70593 Stuttgart, Germany

Covalently cross-linked proteins are among the major modifications caused by the advanced Maillard reaction. So far, the chemical nature of these aggregates is largely unknown. Investigations are reported on the isolation of 6-[2-{[(4*S*)-4-amino-4-carboxybutyl]amino}-6,7-dihydroxy-6,7-dihydroimidazo[4,5-*b*]azepin-4(5*H*)-yl]-L-norleucine (**10**) and *N*-acetyl-6-[(6*R*,7*R*)-2-{[4-(acetylamino)-4-carboxybutyl]amino}-6,7,8a-trihydroxy-6,7,8,8a-tetrahydroimidazo[4,5-*b*]azepin-4(5*H*)-yl]-L-norleucine (**12**) formed by oxidation of the major Maillard cross-link glucosepane **1**. Independent synthesis and unequivocal structural characterization are given for **10** and **12**. Spiro cross-links, representing a new class of glycoxidation products, were obtained by dehydrogenation of the amino imidazolinimine compounds N^6-{2-{[(4*S*)-4-ammonio-5-oxido-5-oxopentyl]amino}-5-[(2*S*,3*R*)-2,3,4-trihydroxybutyl]-3,5-dihydro-4*H*-imidazol-4-ylidene}-L-lysinate (DOGDIC **2**) and N^6-{2-{[(4*S*)-4-ammonio-5-oxido-5-oxopentyl]amino}-5-[(2*S*)-2,3-dihydroxypropyl]-3,5-dihydro-4*H*-imidazol-4-ylidene}-L-lysinate (DOPDIC **3**). These new oxidation products were synthesized, and their unambiguous structural elucidation proved the formation of the spiro imidazolimine structures N^6-[(7*R*,8*S*)-2-{[(4*S*)-4-ammonio-5-oxido-5-oxopentyl]amino}-8-hydroxy-7-(hydroxymethyl)-6-oxa-1,3-diazaspiro[4.4]non-1-en-4-ylidene]-L-lysinate (**16**), N^6-(8*R*,9*S*)-2-{(4*S*)-4-ammonio-5-oxido-5-oxopentyl]amino}-8,9-dihydroxy-6-oxa-1,3-diazaspiro[4.5]dec-1-en-4-ylidene)-L-lysinate (**19**), and N^6-{(8*S*)-2-[(4-amino-4-carboxybutyl)amino]-8-hydroxy-6-oxa-1,3-diazaspiro[4.4]non-1-en-4-ylidene}-L-lysinate (**18**), respectively. It was shown that reaction of the imidazolinone **15** led to the formation of spiro imidazolones, structurally analogous to **16** and **19**.

KEYWORDS: Maillard reaction; glucosepane; spiro cross-links; advanced glycation end product (AGE); advanced glycoxidation end product (AGOE)

INTRODUCTION

The Maillard reaction or "nonenzymatic browning" is a complex series of reactions between reducing carbohydrates with lysine side chains or *N*-terminal amino groups of proteins. The first step of this process is the formation of labile Schiff bases, which rearrange to the more stable Amadori products. The Amadori compounds are slowly degraded in complex reaction pathways via dicarbonyl intermediates to a plethora of compounds (*1*, *2*) subsumed summarily under the term AGEs; this overall reaction sequence proceeds in vitro, in vivo, and in foods. In long-lived tissue proteins, such as collagen and eye lens crystallins, these chemical modifications accumulate with age and may contribute to pathophysiologies associated with aging and long-term complications of diabetes and atherosclerosis. Among these, reactions leading to inter- or intramolecular protein cross-linking are of special importance for the nutritional and functional properties of various foods (*3*). A major consequence of the advanced Maillard reaction is the formation of covalently cross-linked proteins. On the basis of various model reactions, different mechanisms for cross-linking of amino acid side chains in proteins have been discussed (*4*–*15*). So far, pentosidine **8** (*16*), fluorophore LM-1 (*17*, *18*), crossline (*19*), MOLD **6** (*20*), and GOLD **7** (*21*, *22*) have been detected in vivo. We have shown previously that the lysine–arginine cross-links glucosepane **1**, **2**, MODIC **4**, and GODIC **5** (**Figure 1**) represent major Maillard cross-links in vivo (*23*). Trace amounts of the dehydrogenation products **16** and **19** have also been detected in brunescent cataractous lens proteins (*23*). The quantitative results for food samples given for **1**, **2** and **4**, **5** (*3*) are in some cases in the same order of magnitude as those reported for cross-linked amino acids such as lysinoalanine or histidinoalanine (*24*). Some of the cross-links (e.g., fluorophore LM-1, **7**, and **5**) are formed via posttranslational modification of proteins byproducts of carbohydrate oxidation; they can therefore be designated as AGOEs, thus representing a subgroup of AGE. For better understanding the impact of the Maillard reaction on foods and in vivo, it is an absolute prerequisite to establish the chemical nature of the major protein cross-links and to elucidate their formation.

* To whom correspondence should be addressed. Tel: (49)711-4594099. Fax: (49)711-4594096. E-mail: oreihl@uni-hohenheim.de.

10.1021/jf034292+ CCC: $25.00
Published on Web 07/04/2003

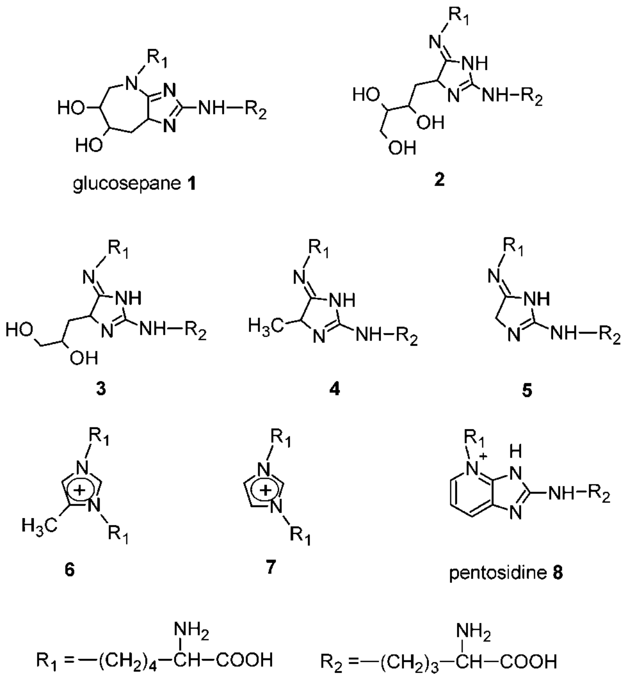

Figure 1. Structural formulas of major protein cross-links: glucosepane **1**, **2**–**7**, and pentosidine **8**.

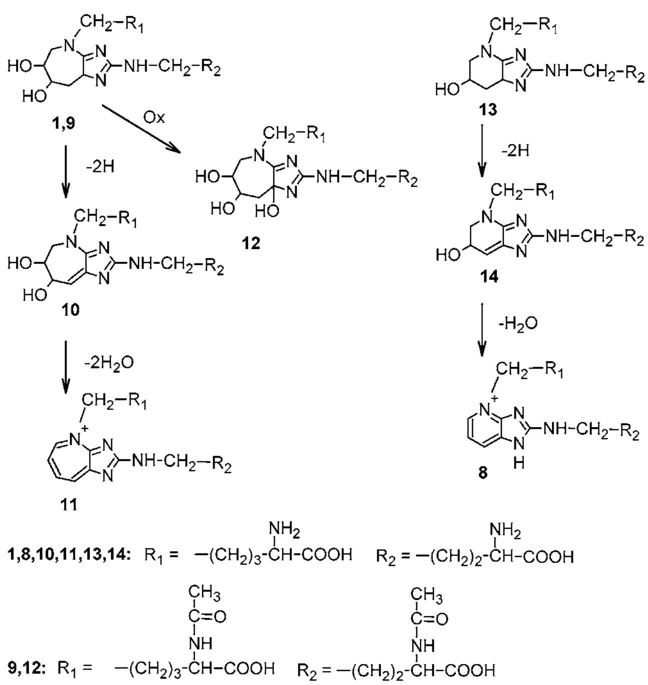

Figure 2. Postulated reaction scheme for the oxidation of glucosepane **1** into **11** via the intermediate **10** and the established reaction scheme for transformation of pentosinane **13** to pentosidine **8** via the intermediate **14**.

We now report on the structural characterization of two oxidation products of glucosepane **1**, 6-[2-{[(4*S*)-4-amino-4-carboxybutyl]amino}-6,7-dihydroxy-6,7-dihydroimidazo[4,5-*b*]azepin-4(5*H*)-yl]-L-norleucine (dehydroglucosepane **10**) and *N*-acetyl-6-[(6*R*,7*R*)-2-{[4-(acetylamino)-4-carboxybutyl]amino}-6,7,8a-trihydroxy-6,7,8,8a-tetrahydro-imidazo[4,5-*b*]azepin-4(5*H*)-yl]-L-norleucine (**12**, **Figure 2**). Additionally, novel spiro cross-links derived from the imidazolimine cross-links **2** and **3** and the imidazolinone **15** were independently synthesized and their structures (**Figure 3**) were unequivocally established as follows: N^6-[(7*R*,8*S*)-2-{[(4*S*)-4-ammonio-5-oxido-5-oxopentyl]amino}-8-hydroxy-7-(hydroxymethyl)-6-oxa-1,3-diazaspiro[4.4]non-1-en-4-ylidene]-L-lysinate (**16**), N^6-((8*R*,9*S*)-2-{(4*S*)-4-ammonio-5-oxido-5-oxopentyl]amino}-8,9-dihydroxy-6-oxa-1,3-diazaspiro[4.5]dec-1-en-4-ylidene)-L-lysinate (**19**), N^6-{(8*S*)-2-[(4-amino-4-carboxybutyl)amino]-8-hydroxy-6-oxa-1,3-diazaspiro[4.4]non-1-en-4-ylidene}-L-lysine (**18**), N^5-[(7*S*,8*R*)-8-hydroxy-7-(hydroxymethyl)-4-oxo-6-oxa-1,3-diazaspiro[4.4]non-1-en-2-yl]-L-ornithine (**17**), and N^5-[(8*R*,9*R*)-8,9-dihydroxy-4-oxo-6-oxa-1,3-diazaspiro[4.5]dec-1-en-2-yl]-L-ornithine (**20**). The aim of the present work was the isolation and structural elucidation of these structures in order to obtain standards for screening in foodstuffs and in vivo.

MATERIALS AND METHODS

Nuclear Magnetic Resonance Spectroscopy (NMR). ^{1}H (500 MHz), ^{1}H,^{1}H-COSY (correlation spectroscopy), ^{1}H,^{1}H-TOCSY (total correlation spectroscopy), TOCSY 1D (one-dimensional), gs-HSQC (gradient-selected heteronuclear single quantum coherence), and gs-HMBC (gradient-selected heteronuclear multiple bond correlation) spectra were recorded at 25 °C on a Varian (Darmstadt, Germany) Unity Inova 500 spectrometer in D_2O.

Liquid Chromatography−Mass Spectrometry (LC-MS). The LC−(ESI; electrospray ionization) MS analyses were run on an HP1100 (Hewlett-Packard, Waldbronn, Germany) high-performance liquid chromatography (HPLC) system coupled to a Micromass (Manchester, U.K.) VG platform II quadrupole mass spectrometer equipped with an ESI interface. The HPLC system consists of an HP1100 autosampler, HP1100 gradient pump, HP1100 thermoregulator, and HP1100 diode array detector module. Column: 150 mm × 4.6 mm i.d., 5 μm, YMC-Pack Pro C 18; 10 mm × 4.6 mm i.d. guard column (YMC Europe, Schermbeck, Germany); column temperature, 25 °C; flow rate, 1.0 mL/min; injection volume, 20 μL. Gradients: 10 mM ammonium formate buffer (pH 4.0)−MeOH. (A) 5% MeOH, 0 min; 95% MeOH, 30−40 min; 5% MeOH, 45−50 min. (B) 5% MeOH, 0 min; 15% MeOH, 10 min; 95% MeOH, 20−25 min; 5% MeOH, 30−35 min. (C) 5% MeOH, 0 min; 15% MeOH, 10 min; 95% MeOH, 15−20 min; 5% MeOH, 24−28 min, 10 mM *n*-heptafluorobutyric acid (HFBA)−MeOH. (D) 5% MeOH, 0 min; 50% MeOH, 25 min; 95% MeOH, 30−35 min; 5% MeOH, 40−47 min. MS parameters: ESI$^+$ source temperature, 120 °C; capillary, 3.5 kV; HV lens, 0.5 kV; cone, 55 V. For LC analyses, the MS system was operated in the full scan mode (*m/z* 150−1000). For accurate mass determination, data were collected in the multichannel acquisition (MCA) mode with 128 channels per *m/z* unit using 12 scans (6 s) with 0.1 s reset time. The resolution was 1060−1110 (10% valley definition). The sample was dissolved in water/MeCN (1:1) containing reference material (0.1 μg/μL, see below), ammonium formate (0.1%), and formic acid (1%); the sample concentration was similar to that of the reference compound. The solution was introduced into the ESI source (80 °C) at a flow rate of 5 μL/min. The following scan ranges and reference peaks were used for calibration: **16** and **19**, *m/z* 385−485; poly(ethylene glycol) 400, *m/z* 388.2547, 415.2543, 432.2809, 459.2805, 476.3071; **18**, *m/z* 350−460; poly(ethylene glycol) 350 monomethyl ether, *m/z* 358.2441, 385.2438, 402.2703, 429.2700, 446.2965; **12**, *m/z* 480−590; poly(ethylene glycol) 550 monomethyl ether, *m/z* 490.3229, 517.3213, 534.3503, 561.3477, 578.3754; **10**, *m/z* 365−465; poly(ethylene glycol) 400, *m/z* 371.2281, 388.2547, 415.2543, 432.2809, 459.2805. MassLynx 3.2 software was used for data acquisition and processing.

Preparative HPLC. The preparative HPLC system consisted of a Kronlab (Sinsheim, Germany) KD200/100SS gradient pump system combined with a Knauer (Berlin, Germany) A0293 variable wavelength detector and a 250 mm × 20 mm i.d., 7 μm, Nucleosil C 18 column with 50 mm × 20 mm i.d. guard column (Kronlab); injection volume, 1.5 mL; flow rate, 18 mL/min. Gradients were applied as follows: ammonium formate buffer (10 mM, pH 4.0)−MeOH. (A) 30% MeOH, 0 min; 70% MeOH, 15 min; 100% MeOH, 16−21 min; 30% MeOH, 24−30 min. (B) 5% MeOH, 0 min; 40% MeOH, 20 min; 100% MeOH, 21−23 min; 5% MeOH, 24−30 min. (C) 0% MeOH, 0 min; 5% MeOH,

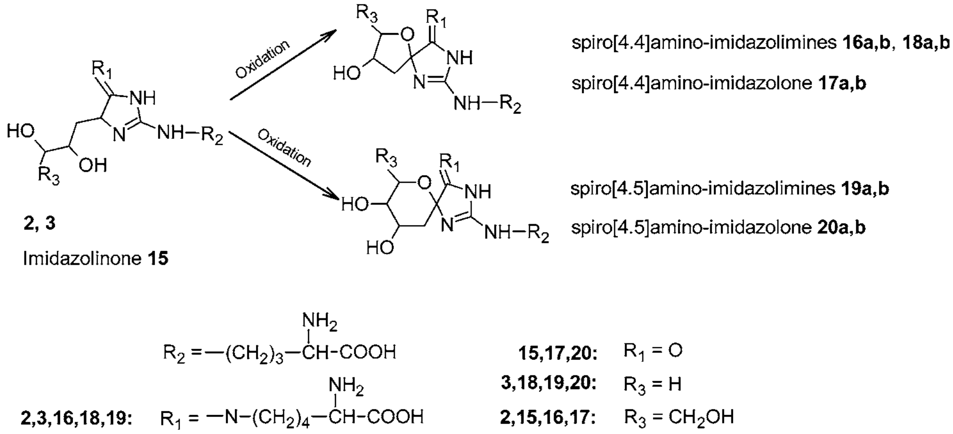

Figure 3. Established reaction scheme for the oxidation of DOGDIC **2**, DOPDIC **3**, and imidazolinone **15**, respectively. Oxidation of **2** yields the spiroamino-imidazolimine structure **16** and **19**; trace amounts of these dehydrogenation products were detected in brunescent lenses. Oxidation of DOPDIC **3** yields the spiroamino-imidazolimine **18**, and oxidation of the imidazolinone **15** yields the spiroamino-imidazolone **17** and **20**.

5−7 min; 0% MeOH, 8−13 min. (D) 0% MeOH, 0 min; 15% MeOH, 10−12 min; 0% MeOH, 13−18 min. (E) 5% MeOH, 0 min; 70% MeOH, 20 min; 100% MeOH, 22−25 min; 5% MeOH, 28−35 min; trifluoroacetic acid (TFA) (0.05%, v/v)−MeOH. (F) 1% MeOH, 0 min; 20% MeOH, 15 min; 100% MeOH, 18−22 min; 1% MeOH, 25−30 min.

Lyophilization. A Leybold-Heraeus (Cologne, Germany) Lyovac GT 2 was used.

Chemicals. Milli-Q water, purified to 18 MΩ/cm^2 (Millipore, Eschborn, Germany), was used in the preparation of all solutions. HPLC grade methanol was employed for LC and LC-MS. For preparative HPLC, solvents were degassed by flushing with helium. N^{α}-*t*-Boc-L-lysine, N^{α}-*t*-Boc-L-arginine, D-glucose, HFBA, and TFA were purchased from Fluka (Neu-Ulm, Germany); poly(ethylene glycol) 350 monomethyl ether, poly(ethylene glycol) 550 monomethyl ether, and poly(ethylene glycol) 400 were from Aldrich (Steinheim, Germany); citric acid and $CuSO_4{\cdot}5H_2O$ were from Merck (Darmstadt, Germany); and N^{α}-acetyl-L-lysine and N^{α}-acetyl-L-arginine were purchased from Bachem (Heidelberg, Germany). For a phosphate buffer with pH 7.4, KH_2PO_4 (2.68 g; 20 mmol) and $Na_2HPO_4{\cdot}H_2O$ (14.3 g; 80 mmol) were mixed vigorously. Glucosepane **1**, **3**, and 3-deoxyglucosone were synthesized according to procedures described previously (*25*−*27*). For a Cu^{2+} citrate solution (100 mM; pH 9), 250 mg of $CuSO_4{\cdot}5H_2O$ and 500 mg of citric acid were dissolved in 10 mL of water; the pH was adjusted by slowly adding solid Na_2CO_3 and $NaHCO_3$.

Synthesis of Dehydroglucosepane 10. Glucosepane **1** (17 mg; 0.04 mmol), $CuSO_4{\cdot}5H_2O$ (1.9 g; 7.5 mmol), and citric acid (3.75 g; 19.5 mmol) were dissolved in 75 mL of water, and the pH adjusted to 9 by slowly adding solid $NaHCO_3$ and Na_2CO_3 and incubated at 70 °C for 6.5 h. The mixture was adjusted to pH 4 with TFA, concentrated to nearly 25 mL by lyophilization, and subjected to preparative HPLC (gradient F; detection wavelength, 280 nm). The fraction with a retention time of 12.9 min yielded, after lyophilization, **10** 3 CF_3COOH (7.3 mg; 0.009 mmol; 24%). LC−(ESI)MS (gradient D): t_R 20.6 min, *m*/*z* 427 [M + H]$^+$. Accurate mass: [M + H]$^+$ calcd for $C_{18}H_{31}N_6O_6$, 427.2305; found, 427.2308 ± 0.009 (mean of 11 measurements ± SD). For NMR data, see **Table 1**.

Synthesis of 12. N^{α}-Acetyl-L-lysine (1.16 g; 6.15 mmol), N^{α}-acetyl-L-arginine (0.9 g; 4.15 mmol), D-glucose (350 mg; 1.95 mmol), and phosphate buffer, pH 7.4 (1.6 g; 9.4 mmol), were dissolved in water (10 mL). The mixture was kept at 70 °C for 17 h and purified by preparative HPLC (gradient E; detection wavelength, 252 nm). Fractions with retention times of 9.1 (F I; 39.3 mg; 0.08 mmol; 4%) and 10.1 min (F II; 42.2 mg; 0.08 mmol; 4%) yielded, after lyophilization, *N*-acetyl-6-[(6*R*,7*R*)-2-{[4-(acetylamino)-4-carboxybutyl]amino}-6,7-dihydroxy-6,7,8,8a-tetrahydroimidazo[4,5-*b*]azepin-4-(5*H*)-yl]-L-norleucine (**9**). LC−(ESI)MS (gradient B): F I, t_R 9.5 min, *m*/*z* 513 [M + H]$^+$; F II, t_R 11.0 min, *m*/*z* 513 [M + H]$^+$.

F I was dissolved in 4 mL of Cu^{2+} citrate (100 mM; pH 9) and kept at 60 °C for 18 h. The mixture was subjected to preparative HPLC (gradient E); the fraction with a retention time of 7.5 min yielded, after lyophilization, **12** HCOOH (1.6 mg; 0.003 mmol; 0.04%). LC−(ESI)-MS (gradient C): t_R 6.1 min, *m*/*z* 529 [M + H]$^+$. Accurate mass: [M + H]$^+$ calcd for $C_{22}H_{37}N_6O_9$, 529.2631; found, 529.2631 ± 0.0008 (mean of 10 measurements ± SD). For NMR data, see **Table 1**.

Synthesis of 16 and 19. N^{α}-*t*-Boc-L-lysine (1.52 g; 6.2 mmol), N^{α}-*t*-Boc-L-arginine (1.15 g; 4.2 mmol), 3-deoxyglucosone (316 mg; ∼48%; 0.9 mmol), and phosphate buffer, pH 7.4 (340 mg; 2 mmol), were dissolved in water (10 mL). The mixture was kept at 60 °C for 48 h and purified by preparative HPLC (gradient A; detection wavelength, 240 nm). Fractions with a retention time of 15.0 min yielded, after lyophilization, N^2-(*tert*-butoxycarbonyl)-N^6-{2-({(4*S*)-4-[(*tert*-butoxycarbonyl)amino]-4-carboxybutyl}amino)-5-[(2*S*,3*R*)-2,3,4-trihydroxybutyl]-3,5-dihydro-4*H*-imidazol-4-ylidene}-L-lysine (*t*-Boc-**2**) HCOOH (80 mg; 0.115 mmol; 13%). LC−(ESI)MS (gradient A): retention time 21.5 min, *m*/*z* 647 [M + H]$^+$. This compound and phosphate buffer, pH 7.4 (34 mg; 0.2 mmol), were dissolved in water (3 mL) and incubated at 50 °C for 48 h. To this solution, 3 mL of aqueous HCl (6 N) was added and kept at ambient temperature for 20 min. The pH was adjusted to 7 by slowly adding solid $NaHCO_3$, and the mixture was subjected to preparative HPLC (gradient D; detection wavelength, 250 nm). Fractions with retention times of 12.7, 13.3, and 14.6 min yielded, after lyophilization, **16a** HCOOH and **19a**,**b** HCOOH (19.3 mg; 0.033 mmol; 3.7%) and **16b** HCOOH (25.6 mg; 0.044 mmol; 4.9%), respectively. LC−(ESI)MS (gradient D): **16a**, retention time 20.8 min, *m*/*z* 445 [M + H]$^+$; **19a**,**b**, retention time 20.9 min, *m*/*z* 445 [M + H]$^+$; **16b**, retention time 21.1 min, *m*/*z* 445 [M + H]$^+$. Accurate mass: **16a** and **19a**,**b** [M + H]$^+$ calcd for $C_{18}H_{33}N_6O_7$, 445.2411; found, 445.2420 ± 0.0008; **16b**: found, 445.2415 ± 0.0010 (mean of nine measurements ± SD). For NMR data, see **Table 2**.

Synthesis of 18. Compound **3** (14 mg; 0.03 mmol) was dissolved in 2 mL of Cu^{2+} citrate (100 mM; pH 9) and kept at 70 °C for 1 h. The mixture was filled up to 4 mL and subjected to preparative HPLC (gradient D; detection wavelength, 252 nm). Fractions with retention times of 10.2 and 11.2 min yielded, after lyophilization, **18a** HCOOH (0.5 mg; 0.001 mmol; 3.8%) and **18b** HCOOH (0.8 mg; 0.002 mmol; 7.7%), respectively. LC−(ESI)MS (gradient D): **18a**, retention time 21.5 min, *m*/*z* 415 [M + H]$^+$; **18b**, retention time 21.8 min, *m*/*z* 415 [M + H]$^+$. Accurate mass: **18a** [M + H]$^+$ calcd for $C_{17}H_{31}N_6O_6$, 415.2305; found, 415.2304 ± 0.0008; **18b**: found, 415.2310 ± 0.0012 (mean of 10 measurements ± SD). For NMR data, see **Table 2**.

Synthesis of 17 and 20. N^{α}-*t*-Boc-L-arginine (274 mg; 1 mmol), 3-deoxyglucosone (325 mg; ∼48%; 1 mmol), and phosphate buffer, pH 7.4 (340 mg; 2 mmol), were dissolved in water (10 mL). The mixture was kept at 50 °C for 5 days and purified by preparative HPLC (gradient B; detection wavelength, 230 nm). Fractions with retention times of 20.2 (F I) and 20.9 min (F II) were isolated and lyophilized. Each fraction was dissolved in aqueous 3 N HCl (1.5 mL) and kept at ambient temperature for 20 min. The pH was adjusted to 7 by slowly adding solid $NaHCO_3$, the volume finally filled up to 3 mL, and the

Table 1. ^{1}H and ^{13}C NMR Data of **10** and **12**[a] in D_2O

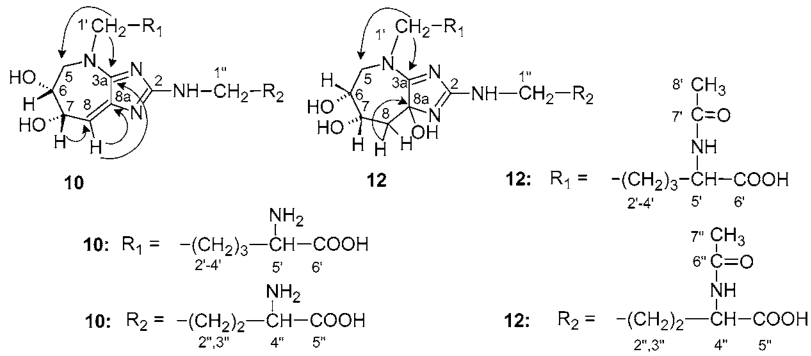

^{1}H NMR	δ (ppm)[b] 10	12	^{13}C NMR	δ (ppm)[b] 10	12
H_A-5	3.76	3.42	C-2	164.7	158.0
H_B-5	3.82	4.26	C-3a	166.9	178.0
H-6	4.11	3.62	C-5	51.5	51.2
H-7	4.40	3.94	C-6	68.5	72.4
H-8	6.18		C-7	69.1	71.6
H_A-8		1.83	C-8	118.5	36.6
H_B-8		2.66	C-8a	134.7	91.2
H_2-1′		3.72	C-1′	54.0	52.8
H_A-1′	3.75		C-2′	27.7	25.8
H_B-1′	3.84		C-3′	22.0	22.1
H_2-2′	1.71	1.76	C-4′	29.9	31.0
H_2-3′	1.43	1.43	C-5′	54.1	55.0
H_2-4′	1.93		C-6′	174.7	179.0
H_A-4′		1.70	C-7′		174.0
H_B-4′		1.88	H_3C-8′		21.7
H-5′	3.84	4.20	C-1″	41.9	41.0
H_3C-8′		2.07	C-2″	24.5	24.2
H_2-1″	3.39	3.35	C-3″	26.5	28.5
H_2-2″	1.75	1.75	C-4″	54.1	54.4
H_2-3″	1.78		C-5″	174.7	179.0
H_A-3″		1.76	C-6″		174.0
H_B-3″		1.87	H_3C-7″		21.7
H-4″	3.84	4.24			
H_3C-7″		2.07			
			J (Hz)[c]		
$^{2}J_{5A,5B}$	(–)14.9	(–)14.3	$^{3}J_{7,8A}$		11.5
$^{2}J_{8A,8B}$		(–)14.3	$^{3}J_{7,8B}$		4.5
$^{3}J_{5A,6}$	4.3	2.0	$^{3}J_{7,8}$	5.4	
$^{3}J_{5B,6}$	5.5	10.6	$^{3}J_{4'A,5'}$		4.9
$^{3}J_{6,7}$	5.9	10.0	$^{3}J_{4'B,5'}$		4.9

[a] The arrows in the structural formulas indicate the characteristic carbon–proton long-range coupling connectivities from the gs-HMBC spectra. Hydrogen/carbon assignment has been validated by $^{1}H,^{1}H$-COSY, TOCSY 1D, gs-HSQC, and gs-HMBC measurements. [b] δ (ppm), chemical shift for the indicated hydrogen/carbon. [c] *J* (Hz), coupling constant between the indicated protons.

mixture was subjected to preparative HPLC (gradient C). Fractions with retention times of 5.6 and 6.3 min resulting from both F I and F II were combined and yielded, after lyophilization, **20a**,**b** HCOOH (3 mg; 0.0083 mmol; 0.83%) and **17a**,**b** HCOOH (5 mg; 0.0138 mmol; 1.38%), respectively. LC−(ESI)MS (gradient D): **20a**,**b**, retention time 12.2 min, *m*/*z* 317 $[M + H]^+$; **17a**,**b**, retention time 12.4 min, *m*/*z* 317 $[M + H]^+$. For NMR data, see **Table 3**.

RESULTS AND DISCUSSION

Formation of the Glucosepane Oxidation Products 10 and 12. We had shown previously (*26*) that the hexose and pentose pathways are differentiated predominantly by the chemical stability of the homologous cross-links glucosepane **1** and pentosinane **13**. While **1** represents a proper AGE under physiological conditions, **13** is smoothly oxidized to **14** (**Figure 2**) and subsequently dehydrated to the AGOE pentosidine **8** (*26*). Glucosepane **1**, established to be of prime quantitative significance in food and in vivo (*3*, *23*), should be dehydrated by the targeted use of oxidants and transformed after double dehydration into the fluorescent heterocycle **11**.

One diastereoisomer of **1** was allowed to react in an alkaline copper(II) citrate buffer for 7 h at 70 °C. The LC−(ESI)MS analysis of the crude reaction mixture showed signals for unreacted **1** and compound **10** ($[M + H]^+$ at *m*/*z* 429 and *m*/*z* 427, respectively) and an additional peak with the quasimolecular ion $[M + H]^+$ at *m*/*z* 445, i.e., 16 Da higher than the $[M + H]^+$ signal for **1**. Because of its high polarity, **10** was very poorly retained on reversed phase material when common eluents were used. The retention behavior was clearly improved if HFBA or TFA was added to the eluent to provide a counterion. Additionally, TFA as well as HFBA are volatile in high vacuum and therefore posed no problems to lyophilization or to the MS system. Thus, the obtained diastereoisomer of **10** with $[M + H]^+$ at *m*/*z* 427 was isolated by preparative HPLC using a TFA−methanol gradient. Accurate mass determination

Table 2. ^{1}H and ^{13}C NMR Data of **16**, **18**, and **19**[a] in D_2O

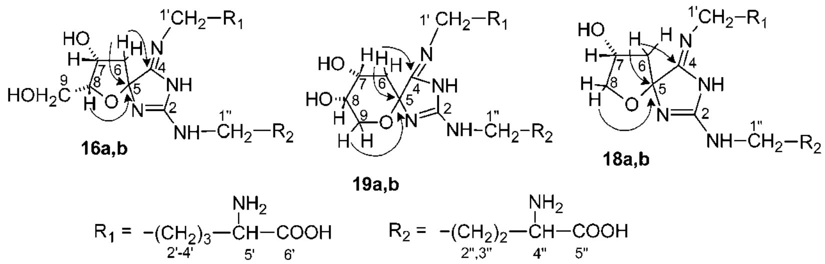

	16a	16b	19a	19b	18a	18b
^{1}H NMR			δ(ppm)[b]			
H_A-6	2.45	2.40	2.03	2.12	2.46	2.50
H_B-6	2.68	2.75	2.21	2.18	2.56	2.63
H-7	4.56	4.57	4.24	4.29	4.75	4.74
H-8	4.30	4.36	4.00	3.83		
H_A-8					4.17	4.08
H_B-8					4.28	4.08
H_A-9	3.63	3.80	3.93	3.83		
H_B-9	3.71	3.80	4.04	3.88		
H_A-1′	3.48	3.48	3.49	3.48	3.49	3.49
H_B-1′	3.48	3.49	3.49	3.48	3.50	3.50
H_2-2′	1.68	1.68	1.70	1.69	1.71	1.71
H_2-3′	1.42	1.44	1.44	1.43	1.44	1.44
H_2-4′	1.86	1.86	1.87	1.86	1.88	1.88
H-5′	3.71	3.71	3.72	3.71	3.72	3.73
H_2-1′′	3.36	3.40	3.41	3.40	3.41	3.38
H_2-2′′	1.71	1.74	1.72	1.71	1.73	1.76
H_2-3′′	1.89	1.90	1.90	1.95	1.92	1.91
H-4′′	3.73	3.76	3.74	3.73	3.77	3.76
			J(Hz)[c]			
$^{2}J_{6A,6B}$	(−)14.9	(−)15.1	(−)13.5	(−)14.6	(−)14.9	(−)15.2
$^{2}J_{8A,8B}$					(−)9.9	
$^{2}J_{9A,9B}$	(−)10.8		(−)13.1	(−)12.3		
$^{2}J_{1'A,1'B}$	*d*	(−)14.2	*d*	*d*	(−)11.0	(−)14.0
$^{3}J_{6A,7}$	3.0	1.8	4.8	3.9	<1	<1
$^{3}J_{6B,7}$	5.3	6.8	12.6	<1	5.0	4.5
$^{3}J_{7,8}$	2–3	2–3	3.0	*d*		
$^{3}J_{7,8A}$					<1	1–2
$^{3}J_{7,8B}$					3.9	1–2
$^{3}J_{8,9A}$	5.8	3.3	<1	12.0		
$^{3}J_{8,9B}$	*d*	3.3	2.2	3.0		
$^{3}J_{1',2'}$	*d*	6.5	*d*	*d*	*d*	7.2
$^{3}J_{4',5'}$	*d*	6.2	*d*	*d*	5.9	5.9
$^{3}J_{1'',2''}$	7.0	6.8	6.9	6.9	6.6	6.6
$^{3}J_{3'',4''}$	6.1	6.1	6.1	6.1	5.9	6.1
^{13}C NMR			δ(ppm)[b]			
C-2	166.9	166.4	167.3	167.3	168.0	168.0
C-4	178.8	179.1	177.8	177.8	179.0	179.0
C-5	100.0	99.3	93.0	*f*	99.0	100.0
C-6	41.0	44.0	34.0	*f*	44.0	42.1
C-7	72.3	72.6	64.5	66.0	71.1	71.8
C-8	89.2	90.8	66.9	65.5	78.0	77.9
C-9	61.7	61.1	68.5	68.8		
C-1′	43.4	42.1	43.3	43.3	43.4	43.4
C-2′	27.8	27.2	27.8	27.8	27.8	27.8
C-3′	22.1	22.1	22.1	22.1	22.1	22.1
C-4′	30.2	30.7	30.2	30.2	30.4	30.4
C-5′	54.8	54.3	54.8	54.8	55.0	55.0
C-6′	175.7	175.7	175.7	175.7	175.2	175.8
C-1′′	42.2	41.8	42.4	42.4	42.4	42.4
C-2′′	24.6	23.8	24.6	24.6	24.2	24.2
C-3′′	27.8	28.1	27.8	27.8	28.0	28.0
C-4′′	54.8	54.1	54.8	54.8	54.8	54.9
C-5′′	175.4	175.2	175.4	175.4	175.0	175.2

[a] The arrows in the structural formulas indicate the characteristic carbon–proton long-range coupling connectivities from the gs-HMBC spectra. No absolute configuration was determined for the diastereoisomers **16** and **19** as well as **18a**,**b**. Hydrogen/carbon assignment has been validated by ^{1}H,^{1}H-COSY, TOCSY 1D, gs-HSQC, and gs-HMBC measurements. [b] δ (ppm), chemical shift for the indicated hydrogen/carbon. [c] *J* (Hz), coupling constant between the indicated protons. [d] No coupling constant can be determined due to overlapping multiplets. [e] Coupling constants were not determined due to higher order spin systems. [f] Chemical shift for C-5 could not be determined due to the lacking connectivity (^{4}J) of HA/B-4/3 or H-6/5 with C-5 in the gs-HMQC spectra and the low amounts available for **19b**.

Table 3. ^{1}H and ^{13}C NMR Data of the Imidazolone **17** and **20**[a] in D_2O

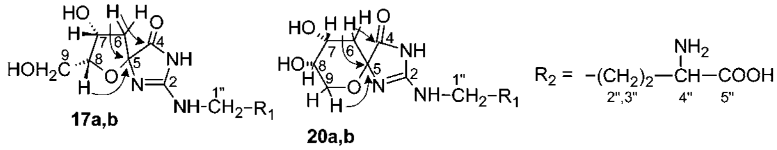

	17a	17b	20a	20b
^{1}H NMR		δ(ppm)[b]		
H_A-6	2.20	2.15	1.99	2.06
H_B-6	2.56	2.48	2.11	2.11
H-7	4.46	4.45	4.32	4.39
H-8	4.24	4.21	3.91	3.91
H_A-9	3.63	3.60	3.81	3.87
H_B-9	3.71	3.65	3.90	4.06
H_2-1′	3.35	3.42	3.42	3.37
H_2-2′	1.73	1.69	1.70	1.73
H_2-3′	1.90	1.90	1.90	1.90
H-4′	3.76	3.75	3.75	3.76
		J (Hz)[c]		
$^{2}J_{6A,6B}$	(–)14.5	(–)14.2	(–)14.3	(–)14.3
$^{2}J_{9A,9B}$	(–)12.3	(–)12.3	(–)12.2	(–)11.3
$^{3}J_{6A,7}$	3.0	2.2	5.5	7.1
$^{3}J_{6B,7}$	6.3	5.7	2.9	3.7
$^{3}J_{7,8}$	3–4	2–3	2.5	3–4
$^{3}J_{8,9A}$	6.3	6.0	10.2	7.5
$^{3}J_{8,9B}$	4.1	4.4	4.5	3.4
$^{3}J_{1',2'}$	6.8	6.8	6.8	6.8
$^{3}J_{3',4'}$	5.7	5.7	6.1	5.8
^{13}C NMR		δ(ppm)[b]		
C-2	169.0	170.0	170.5	169.0
C-4	188.8	189.4	189.5	187.8
C-5	96.0	95.0	87.2	88.8
C-6	42.1	41.9	35.1	34.6
C-7	72.3	72.3	66.2	65.8
C-8	89.0	89.0	66.3	66.3
C-9	63.5	63.5	63.1	64.2
C-1′	41.6	42.4	42.4	41.8
C-2′	24.8	25.2	25.1	24.8
C-3′	28.2	28.2	28.2	28.2
C-4′	55.0	55.0	55.0	55.0
C-5′	175.4	175.4	175.4	175.4

[a] The arrows in the structural formulas indicate the characteristic carbon–proton long-range coupling connectivities from the gs-HMBC spectra. No absolute configuration was determined for the diastereoisomers **17** and **20**. Hydrogen/carbon assignment has been validated by $^{1}H,^{1}H$-COSY, TOCSY 1D, gs-HSQC, and gs-HMBC measurements. [b] δ (ppm), chemical shift for the indicated hydrogen/carbon. [c] *J* (Hz), coupling constant between the indicated protons.

of the obtained compound gave the expected elemental composition $C_{18}H_{31}N_6O_6$; the NMR data compiled in **Table 1** unequivocally proved formation of **10** (**Figure 2**). The mass and UV spectra for the signals involved in the dehydration process confirmed the postulated structures. For the new double bond introduced in **10**, the position is definitely established by the loss of 2 Da from **1** and the 32 nm bathochromic shift for **10** relative to **1**. This can only be rationalized by extension of the chromophoric system.

Because **14** showed almost spontaneous water elimination (*26*) forming the aromatic structure pentosidine **8**, no such behavior could be observed for **10**, even on heating or in the presence of dehydrating agents. In contrast, formation of 6-(2-{[(4*S*)-4-amino-4-carboxybutyl]amino}imidazo[4,5-*b*]azepin-4-ium-4-yl)-L-norleucine (**11**) requires two further dehydration steps, for which reason the desired aromatic heterocycle could not be obtained.

The oxidation product that was 16 Da higher than **1** and $[M + H]^+$ at *m*/*z* 445 was assigned to an analogue of **12** (**Figure 2**). In contrast to dehydroglucosepane **10**, this postulated structure was very difficult to obtain. Reaction of **1** in alkaline copper(II) citrate solution gave a much lower yield for the desired product with $[M + H]^+$ at *m*/*z* 445 as compared to **10**. In addition, the compound proved unstable in the course of work up, especially at low pH values used during the chromatographic purification. Thus, synthesis of **12** was performed using acetylglucosepane **9** for oxidation (**Figure 2**).

Two products with $[M + H]^+$ at *m*/*z* 513 were isolated from the incubation of D-glucose with N^{α}-acetyl-L-lysine and N^{α}-acetyl-L-arginine. The NMR data (not shown) proved the formation of two diastereoisomers of **9**; the data sets for the heterocyclic core were identical with those found for the major diastereoisomers of **1** (*25*). One diastereoisomer of **9** was allowed to react in a Cu^{2+} citrate solution (100 mM; pH 9) for 18 h at 60 °C. Because the protective groups provide fairly good retention on reverse phase, the product with $[M + H]^+$ at *m*/*z* 529 was isolated by preparative HPLC using an ammonium formate buffer−methanol gradient. Accurate mass determination of the obtained compound gave $[M + H]^+$, corresponding to a loss of 2 Da followed by addition of H_2O and an elemental composition of $C_{22}H_{37}N_6O_9$. The NMR data for **12** are given in **Table 1**. The ^{13}C chemical shifts and connectivities definitely proved the outlined structures for **10** and **12** in **Figure 2**.

Formation of the Spiro Structures 16−20 in the Course of Oxidation of 2, 3, and the Imidazolinone 15. As previously shown (*26*), **2** and **3** (**Figure 3**) are formed from the reaction of L-lysine and L-arginine with the respective 3-deoxyglucosone or 3-deoxypentosone (*28*). They belong, together with the corresponding methylglyoxal- and glyoxal-derived structures **4** and **5** (*29*), to the group of amino imidazolinimine cross-links. Related AGEs, as well as their dehydrogenated follow-up products, have already been described (*30*−*33*). They are formed by the reaction of arginine with the corresponding α-diketo compounds and bear an amino imidazolinone core structure. Konishi et al. (*30*) identified 2-(N^{α}-benzoyl-N^{δ}-ornithylamide)-5-(2,3,4-trihydroxybutyl)-4-imidazolone as a stable end product resulting from the dehydrogenation of the benzoyl derivative of **15** (**Figure 3**). The imidazolinone **15** is a major condensation product of 3-deoxyglucosone with arginine and a structural analogue of **2**. Thus, the identification of stable end products formed by the oxidation of the lysine−arginine cross-links **2** and **3** was undertaken.

The synthesis of **16** and **19** was performed by incubation of *t*-Boc-**2** (*26*) in phosphate buffer, pH 7.4, at 50 °C for 2 days. The formation of the imidazolones **17** and **20** was carried out following the previously described procedure by Konishi et al. (*30*). Briefly, 3-deoxyglucosone, N^{α}-*t*-Boc-L-arginine instead of N^{α}-benzoyl-L-arginine amide ($BzArgNH_2$), and phosphate buffer, pH 7.4, were allowed to react at 50 °C for 5 days. The oxidation process was monitored by LC−(ESI)MS analysis of the crude reaction mixtures and signals with $[M + H]^+$ at *m/z* 645 and *m/z* 417 were detected, i.e., 2 Da lower than the *t*-Boc derivatives of **2** and **15** ($[M + H]^+$ at *m/z* 647 and *m/z* 419, respectively; **Figure 3**). The protective groups were cleaved off in acidic medium, and the four diastereoisomers of **16**/**19** and **17**/**20** with $[M + H]^+$ at *m/z* 445 and *m/z* 317, respectively, were purified by preparative HPLC. Accurate mass determination of the obtained compounds gave $[M + H]^+$ confirming the expected elemental composition $C_{18}H_{33}N_6O_7$. The NMR data (**Table 2**) proved the formation of **16** and **19**, existing as a pair of diastereoisimers. Analogously, pairs of diastereoisomers of the related compounds **17** and **20** were isolated and their structures were unequivocally elucidated by NMR (**Table 3**). The ratio of the spiro[4.4]/spiro[4.5] was for the spiro amino imidazolone structures about 2−3, whereas spiro[4.4] dominated by a factor of 6 relative to the spiro[4.5] for the spiro amino imidazolimine compounds. This discrepancy may be a result of steric effects from the lysine moiety. It is noteworthy that **16**/**19** and **17**/**20** were produced as well using stronger oxidizing agents (Cu^{2+}, pH 9) as described below.

Formation of **18** was also possible under the conditions reported for **16** and **19** (phosphate buffer, pH 7.4, 50 °C, 2 days). Because of the very low product amounts obtained after incubation times of more than 7 days, we decided to change the oxidative conditions given above. To obtain **18**, **3** was reacted in a Cu^{2+} citrate buffer solution (pH 9) at 70 °C for 1 h. The LC−(ESI)MS monitored reaction showed the formation of two new signals with $[M + H]^+$ at *m/z* 415, 2 Da lower than the $[M + H]^+$ of **3**. Accurate mass determination of the isolated compounds gave $[M + H]^+$ corresponding to an elemental composition of $C_{17}H_{31}N_6O_6$. The NMR data compiled in **Table 2** showed the formation of **18** existing as a pair of diastereoisomers, **18a**,**b**.

Structural Assignment. Because compounds **10** and **12** (**Figure 2**), as well as the spiro products **16a**,**b**, **17a**,**b**, **18a**,**b**, **19a**,**b**, and **20a**,**b** (**Figure 3**), represent novel AGOEs, a special effort was invested in unequivocally establishing their structures. All gs-HMBC spectra showed only one single cross-peak for the H_2-1″ triplet in the downfield region, i.e., with C-2. The other two cross-peaks connected this proton resonance with the nonhetero-substituted C-2″ and C-3″ of the arginine moiety. Alternative structures with endocyclic N^{δ} nitrogen of the L-arginine side chain, in contrast, would require correlation of H_2-1″ with both quasicarbonyl carbons (C-2 and C-4) or with C-2 and C-5 in a five-membered ring (*29*).

For the glucosepane oxidation products **10** and **12**, ^1H and ^{13}C NMR chemical shifts (*δ*) and coupling constants (*J*) are shown in **Table 1**. The arrows indicate significant carbon−proton long-range coupling across two or three bonds (^2J or ^3J). For both structures, the correlation of CH_2-1′ of the L-lysine side chain with C-3a and C-5 demonstrated the preserved seven-membered ring (*14*, *25*). Significant changes of **10** in comparison to the initial structure of glucosepane **1** could be observed for C-8a (134.7 ppm) and C-8 (118.5 ppm); the downfield shifted resonances relative to **1** can be best rationalized by the introduction of a double bond at this position. Moreover, this assumption is supported by the loss of the stereogenic center of C-8a and the downfield shift of the H-8 doublet by about 4 ppm, due to the anisotropic effect of the double bond. In **12**, the C-8a resonance was shifted downfield (about 32 ppm) relative to **9**. Because of the formal mass increase of 16 Da for **12**, this can only be manifested by the formation of the hemi-aminoacetal structure outlined in **Figure 2**. The characteristic carbon−proton long-range coupling connectivities from the gs-HMBC spectra proved the definite position of the double bond for **10** and the hemi-aminoacetal structure for **12** (**Table 1**).

The conclusion that the difference in the elemental composition (2H) of **2**, the imidazolinone **15**, and **3** (**Figure 3**), relative to their corresponding oxidation products **16**/**19**, **17**/**20**, and **18**, respectively, results from the nucleophilic addition of the hydroxyl group at C-8/C-9 to C-5 is based on the following arguments. The C-5 resonances for the spiro compounds **16**−**20** are shifted downfield (27−40 ppm) as compared to their initial reactants (**2**, **3**, and **15**), which is rationalized best by the transformation of C-5 into an aminoacetal group (**Tables 2** and **3**). All gs-HMBC spectra displayed clear correlation for the protons at C-8 (five-membered rings) or C-9 (six-membered rings) from C-5; this connectivity can only be explained by ring closure. The characteristic carbon−proton long-range coupling connectivities from the gs-HMBC spectra proved the definite formation of the spiro[4.4]amino-imidazolimines **16** and **18**, the spiro[4.5]amino-imidazolimine **19**, the spiro[4.4]amino-imidazolone **17**, and the spiro[4.5]amino-imidazolone **20**.

A new class of glycoxidation products were detected, which are formed by Maillard processes initiated by hexoses and pentoses. Recently, Biemel et al. (*23*) reported the degradation of **2** under physiological conditions (phosphate buffer, pH 7.4, 37 °C). It was proven that **2** was in part transformed into the spiro structures **16** and **19**. Compounds **16** and **19** are formed from **2** via oxidation and thus represent AGOEs; the reaction rate is pH-dependent and negligible at pH <5. The dehydrogenation products **16** and **19** were exemplarily detected in few brunescent lenses in trace amounts, too. According to these results, it is likely that the novel spiro structures **16** and **19** as well as **18** seem to be only minor components as compared to the major Maillard cross-links glucosepane **1**, **2**, **4**, and **5** in vivo (*23*). However, the occurrence of the novel spiro compounds **16**, **18**, and **19** has not been investigated in foodstuffs and biological samples. Therefore, the influence of processing on food proteins as well as the significance in vivo will have to be examined in subsequent studies.

ABBREVIATIONS USED

AGE, advanced glycation end product; AGOE, advanced glycoxidation end product; DOGDIC **2**, N^6-{2-{[(4*S*)-4-ammonio-5-oxido-5-oxopentyl]amino}-5-[(2*S*,3*R*)-2,3,4-trihydroxybutyl]-3,5-dihydro-4*H*-imidazol-4-ylidene}-L-lysinate; DOPDIC **3**, N^6-{2-{[(4*S*)-4-ammonio-5-oxido-5-oxopentyl]amino}-5-[(2*S*)-2,3-dihydroxypropyl]-3,5-dihydro-4*H*-imidazol-4-ylidene}-L-lysinate; GODIC **5**, N^6-(2-{[(4*S*)-4-ammonio-5-oxido-5-oxopentyl]amino}-3,5-dihydro-4*H*-imidazol-4-ylidene)-L-lysinate; GOLD **7**, 6-{1-[(5*S*)-5-ammonio-6-oxido-6-oxohexyl]-imidazolium-3-yl}-L-norleucinate; MODIC **4**, N^6-(2-{[(4*S*)-4-ammonio-5-oxido-5-oxopentyl]amino}-5-methyl-3,5-dihydro-4*H*-imidazol-4-ylidene)-L-lysinate; MOLD **6**, 6-{1-[(5*S*)-5-am-monio-6-oxido-6-oxohexyl]-4-methylimidazolium-3-yl}-L-norleucinate.

ACKNOWLEDGMENT

We are grateful to Dr. J. Conrad and S. Mika, Institute of Chemistry, University of Hohenheim, for recording the NMR spectra.

LITERATURE CITED

(1) Ledl, F.; Schleicher, E. New aspects of the Maillard reaction in foods and in human body. *Angew. Chem., Int. Ed. Engl.* **1990**, *29*, 565−706.
(2) Friedman, M. Food browning and its preventation: An overview. *J. Agric. Food Chem.* **1996**, *44*, 631−653.
(3) Biemel, K. M.; Bühler, H. P.; Reihl, O.; Lederer, M. O. Identification and quantitative evaluation of the lysine-arginine cross-links GODIC, MODIC, DODIC, and glucosepane in foods. *Nahrung/Food* **2001**, *3*, 210−214.
(4) Kato, H.; Shin, D. B.; Hayase, F. 3-Deoxyglucosone cross-links proteins under physiological conditions. *Agric. Biol. Chem.* **1987**, *51*, 2009−2011.
(5) Brinkmann, E.; Wells-Knecht, K. J.; Thorpe, S. R.; Baynes, J. W. Characterization of an imidazolium compound formed by reaction of methylglyoxal and N^{α}-hippuryllysine. *J. Chem. Soc., Perkin Trans. I* **1995**, 2817−2818.
(6) Wells-Knecht, K. J.; Brinkmann, E.; Baynes, J. W. Characterization of an imidazolium salt formed from glyoxal and N^{α}-hippuryllysine: A model for Maillard reaction cross-links in proteins. *J. Org. Chem.* **1995**, *60*, 6246−6247.
(7) Wells-Knecht, K. J.; Zyzak, D. V.; Litchfield, J. E.; Thorpe, S. R.; Baynes, J. W. Mechanism of autoxidative glycosylation: Identification of glyoxal and arabinose as intermediates in the autoxidative modification of proteins by glucose. *Biochemistry* **1995**, *34*, 3702−3709.
(8) Nissl, J.; Pischetsrieder, M.; Klein, E.; Severin, T. Binding of Maillard products to proteins: Formation of pyrrole carbimines. *Carbohydr. Res.* **1995**, *270*, C1−C5.
(9) Glomb, M. A.; Monnier, V. M. Mechanism of protein modification by glyoxal and glycolaldehyde, reactive intermediates of the Maillard reaction. *J. Biol. Chem.* **1995**, *270*, 10017−10026.
(10) Vasan, S.; Zhang, X.; Kapurniotu, A.; Bernhagen, J.; Teichberg, S.; Basgen, J.; Wagle, D.; Shih, D.; Terlecky, I.; Bucala, R.; Cerami, A.; Egan, J.; Ulrich, P. An agent cleaving glucose-derived protein cross-links in vitro and in vivo. *Nature* **1996**, *382*, 275−278.
(11) Nagaraj, R. H.; Portero-Otin, M.; Monnier, V. M. Pyrraline ether cross-links as a basis for protein cross-linking by the advanced Maillard reaction in aging and diabetes. *Arch. Biochem. Biophys.* **1996**, *325*, 152−158.
(12) Buettner, U.; Gerum, F.; Severin, T. Formation of α-amino acid amides and α−hydroxy-acid amides by degradation of sugars with primary amines. *Carbohydr. Res.* **1997**, *300*, 265−269.
(13) Slatter, D. A.; Murray, M.; Bailey, A. J. Formation of a dihydropyridine derivative as a potential cross-link derived from malondialdehyde in physiological systems. *FEBS Lett.* **1998**, *421*, 180−184.
(14) Lederer, M. O.; Gerum, F.; Severin, T. Cross-linking of proteins by Maillard processes−model reactions of D-glucose or methylglyoxal with butylamine and guanidine derivatives. *Bioorg. Med. Chem.* **1998**, *6*, 993−1002.
(15) Skovsted, I. C.; Christensen, M.; Breinholt, J.; Mortensen, S. B. Characterisation of a novel AGE-compound derived from lysine and 3-deoxyglucosone. *Cell. Mol. Biol.* **1998**, *44*, 1159−1163.
(16) Sell, D. R.; Monnier, V. M. Structure elucidation of a senescence cross-link from human extracellular matrix. Implication of pentoses in the aging process. *J. Biol. Chem.* **1989**, *264*, 21597−21602.
(17) Nagaraj, R. H.; Monnier, V. M. Isolation and characterization of a blue fluorophore from human eye lens crystallins: In vitro formation from Maillard reaction with ascorbate and ribose. *Biochim. Biophys. Acta* **1992**, *1116*, 34−42.
(18) Tessier, F.; Obrenovich, M.; Monnier, V. M. Structure and mechanism of formation of human lens fluorophore LM-1. Relationship to vesperlysine A and the advanced Maillard reaction in aging, diabetes, and cataractogenesis. *J. Biol. Chem.* **1999**, *274*, 20796−20804.
(19) Yamaguchi, M.; Nakamura, N.; Nakano, K.; Kitagawa, Y.; Shigeta, H.; Hasegawa, G.; Ienaga, K.; Nakamura, K.; Nakazawa, Y.; Fukui, I.; Obayashi, H.; Kondo, M. Immunochemical quantification of crossline as a fluorescent advanced glycation endproduct in erythrocyte membrane proteins from diabetic patients with or without retinopathy. *Diabetic Med.* **1998**, *15*, 458−462.
(20) Nagaraj, R. H.; Shipanova, I. N.; Faust, F. M. Protein cross-linking by the Maillard reaction. Isolation, characterization, and in vivo detection of a lysine-lysine cross-link derived from methylglyoxal. *J. Biol. Chem.* **1996**, *271*, 19338−19345.
(21) Odani, H.; Shinzato, T.; Usami, J.; Matsumoto, Y.; Brinkmann-Frye, E.; Baynes, J. W.; Maeda, K. Imidazolium cross-links derived from reaction of lysine with glyoxal and methylglyoxal are increased in serum proteins of uremic patients: Evidence for increased oxidative stress in uremia. *FEBS Lett.* **1998**, *427*, 381−385.
(22) Shamsi, F. A.; Nagaraj, R. H. Immunochemical detection of dicarbonyl-derived imidazolium protein cross-links in human lenses. *Curr. Eye Res.* **1999**, *19*, 276−284.
(23) Biemel, K. M.; Friedl, D. A.; Lederer, M. O. Identification and quantification of major Maillard cross-links in human serum albumin and lens protein: Evidence for glucosepane as the dominant compound. *J. Biol. Chem.* **2002**, *277*, 24907−24915.
(24) Friedman, M. Chemistry, biochemistry, nutrition, and microbiology of lysinoalanine, lanthionine, and histidinoalanine in food and other proteins. *J. Agric. Food Chem.* **1999**, *47*, 1295−1319.
(25) Lederer, M. O.; Bühler, H. P. Cross-linking of proteins by Maillard processes−characterization and detection of a lysine-arginine cross-link derived from D-glucose. *Bioorg. Med. Chem.* **1999**, *7*, 1081−1088.
(26) Biemel, K. M.; Reihl, O.; Conrad, J.; Lederer, M. O. Formation pathways for lysine-arginine cross-links derived from hexoses and pentoses by Maillard processes: Unraveling the structure of a pentosidine precursor. *J. Biol. Chem.* **2001**, *276*, 23405−23412.
(27) Madson, M. A.; Feather, M. S. An improved preparation of 3-deoxy-D-erythro-hexos-2-ulose via the bis(benzoylhydrazone) and some related constitutional studies. *Carbohydr. Res.* **1981**, *94*, 183−191.
(28) Glomb, M. A. Synthese, Strukturaufklärung und Nachweis reaktiver Pentoseabbauprodukte, Ph.D. Thesis, University of Stuttgart, Germany, 1992.
(29) Lederer, M. O.; Klaiber, R. G. Cross-linking of proteins by Maillard processes: Characterization and detection of a lysine-arginine cross-links derived from glyoxal and methylglyoxal. *Bioorg. Med. Chem.* **1999**, *7*, 2499−2507.

(30) Konishi, Y.; Hayase, F.; Kato, H. Novel imidazolone compound formed by the advanced Maillard reaction of 3-deoxyglucosone and arginine residues in proteins. *Biosci., Biotechnol., Biochem*. **1994**, *58*, 1953−1955.
(31) Hayase, F.; Koyama, T.; Konishi, Y. Novel dehydrofuroimidazole compounds formed by the advanced Maillard reaction of 3-deoxy-D-hexos-2-ulose and arginine residues in proteins. *J. Agric. Food Chem.* **1997**, *45*, 1137−1143.
(32) Henle, T.; Walter, A. W.; Haessner, R.; Klostermeyer, H. Detection and identification of a protein-bound imidazolone resulting from the reaction of arginine residues and methylglyoxal. *Z. Lebensm. Unters. Forsch.* **1994**, *199*, 55−58.
(33) Lo, T. W. C.; Westwood, M. E.; McLellan, A. C.; Selwood, T.; Thornalley, P. J. Binding and modification of proteins by methylglyoxal under physiological conditions. A kinetic and mechanistic study with *N*-alpha-acetylarginine, *N*-alpha-acetylcysteine, and *N*-alpha-acetyllysine, and bovine serum albumin. *J. Biol. Chem.* **1994**, *269*, 32299−32305.

Received for review March 25, 2003. Revised manuscript received June 3, 2003. Accepted June 6, 2003.

JF034292+